



# Impact of interannual variations in sources of insoluble aerosol species on orographic precipitation over California's central Sierra Nevada

J. M. Creamean<sup>1,2,\*</sup>, A. P. Ault<sup>2,\*\*</sup>, A. B. White<sup>1</sup>, P. J. Neiman<sup>1</sup>, F. M. Ralph<sup>3,\*\*\*</sup>, P. Minnis<sup>4</sup>, and K. A. Prather<sup>2,3</sup>

<sup>1</sup>NOAA Earth System Research Laboratory, Physical Sciences Division, 325 Broadway St., Boulder, CO 80304, USA

<sup>2</sup>Department of Chemistry and Biochemistry, University of California, San Diego, 9500 Gilman Dr., La Jolla, CA 92093, USA

<sup>3</sup>Scripps Institution of Oceanography, University of California, San Diego, 9500 Gilman Dr., La Jolla, CA 92093, USA

<sup>4</sup>NASA Langley Research Center, 21 Langley Blvd., Hampton, VA 23681, USA

\* now at: Cooperative Institute for Research in Environmental Sciences, University of Colorado at Boulder, Box 216 UCB, Boulder, CO 80309, USA

\*\* now at: Department of Environmental Health Sciences and Department of Chemistry, University of Michigan, 500 S State St., Ann Arbor, MI 48109, USA

\*\*\* now at: Scripps Institution of Oceanography, University of California, San Diego, La Jolla, CA, USA

Correspondence to: K. A. Prather (kprather@ucsd.edu)

Received: 8 December 2014 – Published in Atmos. Chem. Phys. Discuss.: 12 January 2015

Revised: 18 May 2015 – Accepted: 27 May 2015 – Published: 15 June 2015

**Abstract.** Aerosols that serve as cloud condensation nuclei (CCN) and ice nuclei (IN) have the potential to profoundly influence precipitation processes. Furthermore, changes in orographic precipitation have broad implications for reservoir storage and flood risks. As part of the CalWater field campaign (2009–2011), the variability and associated impacts of different aerosol sources on precipitation were investigated in the California Sierra Nevada using an aerosol time-of-flight mass spectrometer for precipitation chemistry, S-band profiling radar for precipitation classification, remote sensing measurements of cloud properties, and surface meteorological measurements. The composition of insoluble residues in precipitation samples collected at a surface site contained mostly local biomass burning and long-range-transported dust and biological particles (2009), local sources of biomass burning and pollution (2010), and long-range transport (2011). Although differences in the sources of insoluble residues were observed from year to year, the most consistent source of dust and biological residues were associated with storms consisting of deep convective cloud systems with significant quantities of precipitation initiated in the ice phase. Further, biological residues were dominant (up to 40 %) during storms with relatively warm cloud

temperatures (up to  $-15^{\circ}\text{C}$ ), supporting the important role bioparticles can play as ice nucleating particles. On the other hand, lower percentages of residues from local biomass burning and pollution were observed over the three winter seasons (on average 31 and 9 %, respectively). When precipitation quantities were relatively low, these insoluble residues most likely served as CCN, forming smaller more numerous cloud droplets at the base of shallow cloud systems, and resulting in less efficient riming processes. Ultimately, the goal is to use such observations to improve the mechanistic linkages between aerosol sources and precipitation processes to produce more accurate predictive weather forecast models and improve water resource management.

## 1 Introduction

Aerosol particles serve as nuclei upon which cloud droplets and ice crystals form and thus can have profound impacts on climate. In particular, pollution aerosols in high number concentrations have been suggested to slow down cloud drop coalescence and accretion by creating large populations of

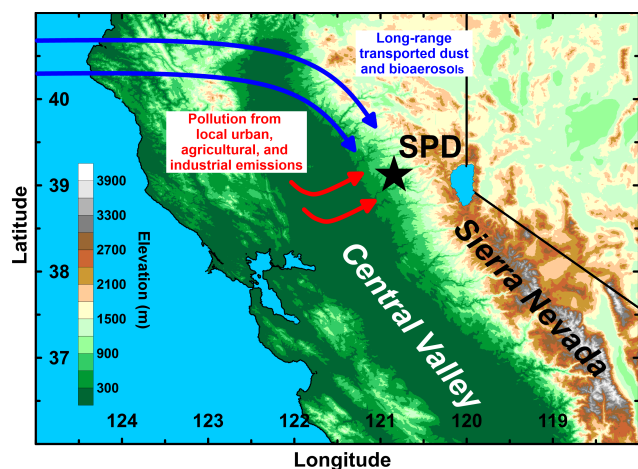


**Figure 1.** Map showing potential aerosol sources and the topography in the region surrounding Sugar Pine Dam (SPD), where precipitation sample collection and meteorological measurements occurred during CalWater.

small-sized cloud droplets that delay the conversion of cloud water into precipitation (Borys et al., 2000; Rosenfeld et al., 2008). In contrast, aerosols that form ice nuclei (IN), such as mineral dust and biological aerosols, have been shown to enhance precipitation via secondary ice formation and aggregation (Bergeron, 1935; Hosler et al., 1957; DeMott et al., 2003; Morris et al., 2004; Tobo et al., 2013). Once formed, crystals can develop rime after colliding with supercooled cloud droplets ( $\geq 10 \mu\text{m}$ ; Yuter and Houze, 2003), particularly in more turbulent clouds (Pinsky et al., 1998). In regions with orographically enhanced cloud formation such as California's Sierra Nevada (Pandey et al., 1999), IN are theorized to become incorporated into the top of high-altitude clouds to form ice crystals (Meyers et al., 1992), whereas cloud condensation nuclei (CCN) have been hypothesized to enhance cloud droplet formation at the base of orographic clouds (Rosenfeld et al., 2008). Under subfreezing conditions, a precipitating ice cloud overlaying a pristine marine liquid water cloud enables growth of precipitation particles through riming via the seeder–feeder process (Choulaton and Perry, 1986; Saleeby et al., 2009). However, if the lower cloud contains high concentrations of CCN, such as those from pollution (Rosenfeld, 2000), ice crystal riming efficiency is reduced and snow growth rates and deposition location are altered (Saleeby et al., 2009). Although the effects of CCN on precipitation suppression in the Sierra Nevada are well documented (Colle and Zeng, 2004; Givati and Rosenfeld, 2004; Rosenfeld and Givati, 2006), the combined effects of CCN and IN simultaneously on precipitation in mixed-phase clouds are not well established (Muhlbauer et al., 2010). It is plausible that these effects can offset one another to some degree, and thus past measurement campaigns that addressed one or the other could not account for the combined effects.

The Sierra Nevada region is influenced by numerous sources of CCN, including regional transport from biomass burning, urban, agricultural, and industrial emissions from the Central Valley (Collett et al., 1990; Guan et al., 2010) in addition to in situ formation of particles that act as CCN from transported gas-phase species (Lunden et al., 2006; Creamean et al., 2011) (see Fig. 1). In contrast, IN populations have been shown to be influenced by dust transported over long distances from arid regions in Africa and Asia (McKendry et al., 2007; Ault et al., 2011; Uno et al., 2011; Creamean et al., 2013, 2014b). Furthermore, biological species (e.g., bacteria) have been shown to be more effective IN (Despres et al., 2012; Murray et al., 2012; O'Sullivan et al., 2014) since they activate at temperatures as warm as  $-1^\circ\text{C}$  (Morris et al., 2004) compared to dust ( $\sim -38$  to  $-17^\circ\text{C}$ ) (Field et al., 2006; Marcolli et al., 2007). Conen et al. (2011) demonstrated that even biological fragments such as proteins can largely determine ice nucleation properties of soil dust in a laboratory setting, while Pratt et al. (2009) observed biological IN in ice residues from one orographic cloud via in situ aircraft measurements. Precipitation events in the Sierra Nevada are influenced largely by the combined effects of transient synoptic-scale dynamics and terrain-locked orographic lift. Ralph et al. (2013a) demonstrated that precipitation totals in land-falling atmospheric rivers (Ralph et al., 2004) depend considerably on orographic lift associated with water vapor transport during storms that move across the California Coast Ranges. Their study showed that differences in storm-total water vapor transport directed up the mountain slope contributed 74 % of the variance in storm-total rainfall across 91 storms from 2004 to 2010. One hypothesis is that the remaining 26 % variance results from influences by other processes, including aerosol impacts on precipitation, as well as convection, synoptic and frontally forced precipitation and static stability. Aircraft and ground-based cloud seeding experiments in the Sierra Nevada suggest aerosols serving as IN are more frequently removed by forming ice crystals versus scavenging during snowfall and increase precipitation rates by  $0.1\text{--}1.0 \text{ mm h}^{-1}$  (Reynolds and Dennis, 1986; Deshler and Reynolds, 1990; Warburton et al., 1995). Frozen winter precipitation in the Sierra Nevada produces a deep snowpack which gradually feeds reservoirs in the spring (Dettinger et al., 2011). However, the presence of CCN may also influence the snowpack by creating smaller cloud droplets that are scavenged less efficiently by falling cloud ice crystals in the riming process, leading to reduced snowfall and thus significant implications for water resources (Borys et al., 2000; Saleeby et al., 2009). In short, the interplay between CCN and IN activity of aerosols and their impacts on precipitation in this region will influence the depth of the Sierra Nevada snowpack and, thus, the water resources available to California.

CalWater (<http://www.esrl.noaa.gov/psd/calwater/overview/calwater1.html>) was a field campaign designed to

study aerosol–cloud–precipitation interactions in California during winter storms, as well as the dynamics of the inland penetration of atmospheric rivers from the coast. A unique combination of radar technology, ground-based aerosol measurements, and hydrometeorological sensors were stationed in the Sierra Nevada and nearby for up to 6 weeks during each of the three winter seasons from 2009 to 2011. This study focuses on identifying cloud seeds, interstitial aerosol, and scavenged aerosols in Sierra Nevada precipitation by examining individual particles as insoluble residues in precipitation samples collected at a ground-based site co-located with a precipitation radar and other meteorological sensors. Key elements of the unique hydrometeorological measurement network were obtained as part of the National Oceanic and Atmospheric Administration’s (NOAA) Hydrometeorology Testbed (Ralph et al., 2013b). Precipitation composition studies regarding the insoluble components were employed for a number of CalWater events by Ault et al. (2011) and Creamean et al. (2013), providing valuable insight into the potential sources of aerosols acting as CCN and IN.

This study probes two unresolved questions from the previous 2009 and 2011 studies by Ault et al. (2011) and Creamean et al. (2013), respectively: (1) how do both local pollution (i.e., from Sierra Nevada and Central Valley) and long-range-transported sources of the insoluble components of aerosols vary between winter seasons? (2) How do these sources impact precipitation processes? This study focuses on measurements from the 2010 winter season in addition to demonstrating the large interannual variability in sources of insoluble residues in the Sierra Nevada during all three winter field seasons, including both long-range-transported and local emissions. Further, we evaluate how these sources impact precipitation formation through comparing the comprehensive set of cases and relating these to radar-observed precipitation characteristics. The links obtained here between sources of the insoluble components of aerosols and precipitation outcomes will ultimately be used as inputs into regional climate models to develop a longer-term mechanistic picture for how different aerosol sources influence clouds and precipitation processes in California.

## 2 Measurements

### 2.1 CalWater field campaign

The CalWater study centered at Sugar Pine Dam (SPD; 1064 m a.s.l.; 39.13° N, 120.80° W; shown in Fig. 1) involved a unique combination of meteorological (NOAA) and atmospheric measurements (University of California, San Diego; UCSD) to deconvolute how different factors affect precipitation quantity and type. Simultaneous atmospheric and meteorological measurements were made from 22 February to 11 March 2009, 27 January to 15 March 2010, and 28 Jan-

uary to 8 March 2011. Dates, times, and analysis statistics for each of the precipitation samples collected during the storms from 2009 to 2011 at SPD are provided in Table 1. Multi-year measurements provide an extensive data set to determine the impact different aerosol sources have during winter storms in California.

### 2.2 Surface meteorology and cloud properties above SPD

Hourly precipitation rates ( $\text{mm h}^{-1}$ ) and 2 min temperature ( $^{\circ}\text{C}$ ) at SPD were acquired from NOAA’s Hydrometeorological Testbed Network (NOAA HMT-West). Storm-total precipitation represents the total accumulated precipitation per storm throughout the CalWater winter sampling season (provided in Table 1). NOAA’s S-band profiling radar (S-PROF; White et al., 2000), a fixed dish antenna, was operated at 2875 MHz and directed vertically to study the backscatter of energy from hydrometeors and cloud droplets and to monitor the radar brightband melting layer (White et al., 2003). The S-PROF radar can distinguish between different precipitation process types by detecting a “brightband”, where the phase of falling precipitation changes from solid to liquid (White et al., 2002). The accumulation and percentages of precipitation process type including non-brightband rain (NBB rain), brightband rain (BB rain), and snow/graupe/hail (herein simply referred to as “snow”) were estimated using the rainfall process-partitioning algorithm developed by White et al. (2003, 2010), which was applied to the S-PROF profiles. These measurements represent the types of precipitation aloft, not just at the surface level. Both snow and BB rain were formed in the ice phase; however, BB rain reached the surface by passing through a melting layer. NBB rain is precipitation that likely originated as liquid droplets and is characterized by a larger number of small drops than BB rain (White et al., 2003; Neiman et al., 2005; Martner et al., 2008). Echo top heights (km a.m.s.l) were also estimated using S-PROF radar data using methods employed by Neiman et al. (2005) and Martner et al. (2008) and used to determine the depth of the clouds above SPD. Analysis was performed on all 30 min periods when the precipitation rate exceeded  $\sim 1 \text{ mm h}^{-1}$ .

Data from the 11th Geostationary Operational Environmental Satellite (GOES-11) were used to define effective cloud temperature, which is close to the cloud-top temperature, and the cloud-top phase over SPD. GOES-11 was centered at 135° W over the eastern Pacific Ocean. Cloud properties from 22 February to 4 March 2009, 27 January to 13 March 2010, and 28 January to 8 March 2011 were retrieved for CalWater. The five channels on the GOES-11 imager include a visible channel ( $0.65 \mu\text{m}$ ), which was calibrated to the Aqua MODIS  $0.64 \mu\text{m}$  channel, as well as four infrared channels. The 4 km pixel GOES-11 data were analyzed each hour for a domain bounded by 30–42.5° N latitude and 112.5–130° W longitude using the methods de-

**Table 1.** Statistics for precipitation sample collection during storms from 2009 to 2011 at SPD. The start and end dates reflect when the beakers were placed outside; they do not always correspond to the exact start and end of falling precipitation. The percentages of each insoluble residue type per sample are provided (bolded percentages show dominant type).

Year	Storm	Precip. total (mm)	Sample ID	Start (UTC)	End (UTC)	# of residues	Dust	Biological	Biomass burning	Pollution	Other		
2009	1	84	S1	22 Feb 19:30	23 Feb 18:45	399	11 %	17 %	<b>70 %</b>	2 %	0 %		
			S2	23 Feb 18:45	24 Feb 19:20	70	<b>38 %</b>	19 %	31 %	11 %	0 %		
	2	14	S3	26 Feb 00:00	26 Feb 19:45	236	16 %	5 %	<b>76 %</b>	3 %	0 %		
			3	158	S4	1 Mar 16:00	2 Mar 01:30	6252	6 %	0 %	<b>79 %</b>	15 %	1 %
	S5	2 Mar 01:30			2 Mar 04:30	505	23 %	0 %	<b>77 %</b>	0 %	0 %		
	S6	2 Mar 05:20			2 Mar 20:20	749	<b>46 %</b>	1 %	46 %	0 %	7 %		
	S7	2 Mar 20:20			3 Mar 01:45	251	<b>49 %</b>	2 %	45 %	0 %	3 %		
	S8	3 Mar 05:20			3 Mar 18:20	547	<b>72 %</b>	4 %	19 %	2 %	4 %		
	S9	3 Mar 18:45			4 Mar 01:00	253	<b>79 %</b>	4 %	8 %	0 %	9 %		
	S10	4 Mar 01:00			4 Mar 12:00	82	<b>80 %</b>	9 %	0 %	6 %	5 %		
2010	4	23			S11	27 Jan 01:00	31 Jan 01:00	153	21 %	<b>44 %</b>	20 %	14 %	1 %
			5	37	S12	3 Feb 03:00	3 Feb 21:00	134	<b>31 %</b>	22 %	26 %	19 %	2 %
	S13	4 Feb 19:15			5 Feb 17:45	119	11 %	29 %	<b>45 %</b>	13 %	2 %		
	S14	5 Feb 17:45			6 Feb 23:00	29	3 %	17 %	<b>41 %</b>	38 %	0 %		
	6	27			S15	20 Feb 02:45	20 Feb 17:45	460	13 %	19 %	<b>37 %</b>	29 %	2 %
			S16	21 Feb 03:25	21 Feb 17:15	643	12 %	25 %	<b>53 %</b>	8 %	2 %		
			S17	21 Feb 17:15	22 Feb 18:06	405	19 %	30 %	<b>37 %</b>	12 %	2 %		
	7	56	S18	23 Feb 22:30	24 Feb 17:15	79	10 %	20 %	<b>61 %</b>	5 %	4 %		
			8	60	S19	26 Feb 18:45	27 Feb 00:00	225	23 %	31 %	<b>32 %</b>	10 %	4 %
	S20	27 Feb 00:00			27 Feb 06:15	351	4 %	34 %	<b>54 %</b>	5 %	3 %		
	S21	27 Feb 06:15			27 Feb 17:20	46	33 %	26 %	<b>33 %</b>	4 %	4 %		
	9	56			S22	2 Mar 14:45	3 Mar 03:00	190	21 %	25 %	<b>40 %</b>	12 %	3 %
					S23	3 Mar 03:00	3 Mar 19:00	444	20 %	20 %	<b>51 %</b>	8 %	1 %
					S24	3 Mar 19:00	4 Mar 02:00	245	29 %	29 %	<b>35 %</b>	3 %	4 %
	10	24	S25	4 Mar 02:00	4 Mar 19:00	487	11 %	<b>55 %</b>	29 %	4 %	1 %		
			S26	8 Mar 16:00	9 Mar 00:40	497	9 %	36 %	18 %	<b>34 %</b>	3 %		
			S27	9 Mar 00:40	9 Mar 16:00	253	16 %	<b>51 %</b>	24 %	6 %	2 %		
	11	37	S28	9 Mar 16:00	10 Mar 20:30	461	11 %	33 %	<b>43 %</b>	13 %	0 %		
S29			12 Mar 18:15	12 Mar 23:15	239	<b>33 %</b>	28 %	30 %	10 %	0 %			
S30			12 Mar 23:15	13 Mar 05:00	376	30 %	16 %	<b>45 %</b>	8 %	0 %			
S31			13 Mar 05:00	13 Mar 17:30	299	21 %	27 %	<b>35 %</b>	17 %	0 %			
2011	12	41	S32	30 Jan 02:53	30 Jan 20:00	130	<b>55 %</b>	21 %	15 %	5 %	4 %		
			13	84	S33	14 Feb 18:40	15 Feb 17:00	360	<b>44 %</b>	8 %	16 %	6 %	26 %
	S34	15 Feb 17:05			16 Feb 18:00	266	<b>66 %</b>	7 %	10 %	1 %	17 %		
	14	83			S35	16 Feb 19:45	17 Feb 17:30	233	<b>94 %</b>	6 %	1 %	0 %	0 %
					S36	17 Feb 17:30	18 Feb 18:40	208	<b>78 %</b>	20 %	1 %	0 %	1 %
	15	77	S37	18 Feb 19:15	19 Feb 18:40	163	<b>71 %</b>	12 %	1 %	3 %	14 %		
			S38	24 Feb 20:30	26 Feb 21:00	94	12 %	<b>83 %</b>	1 %	4 %	0 %		
			16	30	S39	1 Mar 23:00	2 Mar 23:00	26	<b>73 %</b>	15 %	0 %	8 %	4 %
	S40	2 Mar 23:00			3 Mar 19:00	398	27 %	<b>37 %</b>	18 %	18 %	0 %		
	17	52	S41	5 Mar 21:00	6 Mar 18:15	351	38 %	<b>50 %</b>	5 %	6 %	1 %		
S42			6 Mar 18:15	7 Mar 18:00	204	29 %	<b>40 %</b>	15 %	13 %	2 %			

scribed by Minnis et al. (2008, 2011). Data from all parallax-corrected pixels within a 10 km radius of the SPD were used to compute mean effective cloud temperature and percentage of cloud ice.

### 2.3 Analysis of insoluble precipitation residue particles and ambient aerosols

Methods for collection and analysis of insoluble precipitation residues are described elsewhere (Holecck et al., 2007; Ault et al., 2011; Creamean et al., 2013, 2014a). Briefly, precipita-

tion samples were manually collected using beakers cleaned with ultrapure Milli-Q water ( $18\text{ M}\Omega\text{ cm}^{-1}$ ) and methanol. Most samples were analyzed immediately after collection, while others were transferred to 500 mL glass bottles, frozen, and stored for 6–10 days before chemical analysis. Insoluble residues in the precipitation samples were resuspended using a Collision atomizer, dried using two silica gel diffusion driers, and sampled by an aerosol time-of-flight mass spectrometer (ATOFMS) (Gard et al., 1997). This aerosolization method can produce single soluble and insoluble particles, agglomerates of different particle types, and coatings of soluble species on insoluble residues. Thus, the composition is likely somewhat altered from how the particles would have existed in the atmosphere (Holecek et al., 2007). Even with the caveats associated with the aerosolization process as discussed in Creamean et al. (2013, 2014a), this method provides useful information on chemical differences in the aerosols seeding clouds.

Insoluble precipitation residues between 0.2 and 3.0  $\mu\text{m}$  in diameter were individually sized and chemically analyzed by the ATOFMS. In this instrument, single particles traverse between and scatter the light from two continuous wave lasers (532 nm) at a set distance apart from which particle size is calculated based on particle velocity upon calibration using known size polystyrene latex spheres. A third pulsed Nd:YAG laser (266 nm) is then triggered and simultaneously desorbs and ionizes each sized particle, generating positive and negative ions which are analyzed using a dual-polarity time-of-flight mass spectrometer. The mass spectra from individual particles were classified into different types based on combinations of characteristic ion peaks as discussed in detail by Creamean et al. (2014a). Peak identifications correspond to the most probable ions for a given mass-to-charge ( $m/z$ ) ratio based on previous ATOFMS precipitation studies (Holecek et al., 2007; Ault et al., 2011; Creamean et al., 2013, 2014a).

Ambient aerosols were analyzed using ATOFMS simultaneous to precipitation sample collection time periods. The instrument operates in the same manner as with the insoluble residues; however, ambient air was drawn into the inlet instead of resuspended particles from atomized precipitation samples. Due to the sheer number of ambient aerosols analyzed by ATOFMS, particles were classified via a clustering algorithm as opposed to hand classification. Single-particle mass spectra were imported into YAADA (Allen, 2004), a software toolkit in MATLAB (The MathWorks Inc.), for detailed analysis of particle size and chemistry. ART-2a, an adaptive resonance theory-based clustering algorithm (Song et al., 1999), was then used to classify particles into separate groups depending on the presence and intensity of ion peaks within an individual particle's mass spectra. The most populated 50–70 clusters accounted for > 90 % of the total ART-2a classified particles and are considered representative of the overall aerosol composition. Peak identifications within this paper correspond to the most probable ions for a given

mass-to-charge ratio. The same ART-2a algorithm was applied to the precipitation residues; the residue percentages per sample for each particle type were within 6–10 % of the manually classified results. Thus, the ambient and precipitation residues, although classified by different methods, are comparable to each other.

### 3 Results and discussion

#### 3.1 Interannual variability of precipitation residue composition measured by ATOFMS

The insoluble residue chemical composition during the three winter sampling seasons was mainly composed of dust, biological material, and organic carbon (OC). The OC residues were predominantly from biomass burning (Ault et al., 2011; Creamean et al., 2014a), with minor contributions from agricultural and pollution aerosols from the Central Valley (hereafter referred to simply as “pollution”) (McGregor and Anastasio, 2001; Gaston et al., 2013). Mass spectra for each of these types are shown by Creamean et al. (2013, 2014a) and Ault et al. (2011). Other types contributed to  $\leq 8\%$  of the total residues each year. Control experiments of specific mixtures and solutions – including dust, leaf litter, smoke, and sea salt – were conducted using ATOFMS to accurately identify residue types observed in precipitation samples. These are discussed in detail by Creamean et al. (2014a), in addition to the chemical speciation of the major residue types from precipitation samples. The ATOFMS is less sensitive to soluble species, such as sea salt, as they form residues that are too small to detect and chemically analyze when concentrations are low due to dilution that occurs in precipitation samples (Creamean et al., 2014a). Briefly, in ATOFMS analysis, dust particles typically contain a combination of different metal and metal oxides, including but not limited to aluminosilicates, iron, and titanium. Biological residues typically contain a combination of sodium, magnesium, potassium, calcium, organic nitrogen markers, and/or phosphate. In many cases, dust residues were mixed with biological material as indicated by the combination of ion markers. The mixed nature of the dust with biological material is likely a result of soil dust (Conen et al., 2011) or other sources such as dust interacting with marine biomaterial during transport (Prather et al., 2013), and to a lesser extent agglomerates produced during the analysis resuspension process (Creamean et al., 2014a). Thus these mixed particles were grouped into the “dust” category. Biomass burning residues varied in composition but typically contain sodium, potassium, aged organic carbon fragments, high-mass organic carbon markers, and/or polycyclic aromatic hydrocarbon markers. Pollution residues contained aged organic carbon and/or amine markers, with a dearth of common biomass burning markers. Ault et al. (2011) illustrated the ubiquitous presence of local biomass burning in precipitation at SPD during

the 2009 winter sampling and highlighted the potential importance of these aerosols as CCN (Holecek et al., 2007). In particular, biomass burning aerosols containing potassium and sodium have been shown to be hygroscopic in CCN measurements (Carrico et al., 2010; Engelhart et al., 2012). Ault et al. (2011) also suggested the source of the dust in 2009 was from high-altitude, long-range transport as opposed to local or regional sources. Further, Creamean et al. (2013) demonstrated that dust and biological aerosols during the 2011 measurements were long-range-transported particles which became incorporated into the tops of high-altitude clouds. Dust from Asia has been shown to reach the US west coast consistently throughout the late winter/early spring (Husar et al., 2001; VanCuren and Cahill, 2002; Liu et al., 2003; Jaffe et al., 2005; Creamean et al., 2014b).

Large variations existed between the major precipitation residue types during the three winter seasons (Table 1). The results from 2009 were presented in detail by Ault et al. (2011), and therefore will only be briefly discussed here. It is important to note that only two of the three 2009 storms (storms 1 and 3 here) were presented in Ault et al. (2011) due to their meteorological similarities. As shown in Table 1, during storms 1 and 2, the residues were mainly composed of biomass burning (70 and 76 % for samples 1 and 3, denoted “S1” and “S3”, respectively), with some dust present (up to 38 % in S2). However, during storm 3, the residue composition shifted to predominantly dust (46–80 %, S6–S10). Even though meteorological conditions were relatively similar during the most intense storms (storms 1 and 3), the precipitation shifted to snow during storm 3 due to colder conditions later in that event. This storm produced 40 % more precipitation than the first storm (Ault et al., 2011). During the 2010 winter sampling season, high percentages of biomass burning particles were present throughout the entire study (up to 61 %, 38 % on average) and constituted the dominate residue type during almost all of the storms. In contrast, in 2011, dust residues were dominant during the first storms (44–94 %, storms 12–14), while biological percentages were highest during most of the latter storms (37–83 %, storms 15–17). The results from 2011, presented in detail in Creamean et al. (2013), are only briefly discussed. Overall, each winter sampling season was impacted by very different aerosol sources, which we hypothesize impacted the type and quantity of precipitation as discussed in the following section.

Although we cannot determine directly, we hypothesize that the residue types from each winter sampling season were most likely present due to nucleation in cloud with a smaller contribution from scavenging of ambient aerosols during rainfall/snowfall. Figure 2 shows the composition of the precipitation residues compared to the relative abundance of the ambient aerosols present during each sampling time period for 2010 (2009 and 2011 are shown and/or discussed in Ault et al. (2011) and Creamean et al. (2013), respectively). Dust, biomass burning, and pollution were present in both in the ambient aerosol as well as the residues. Sea salt

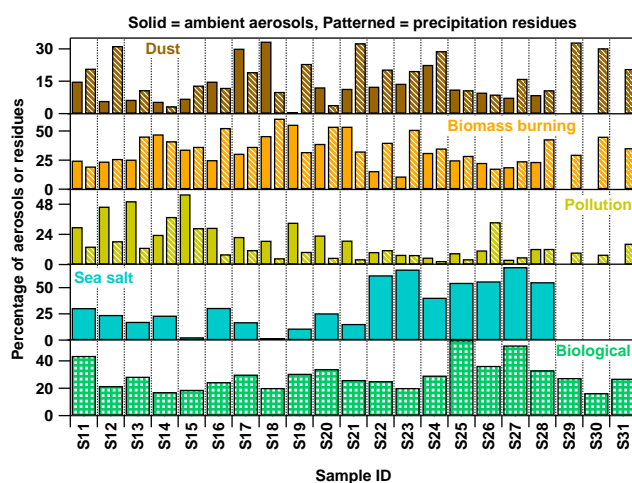


**Figure 2.** Comparison of average ambient aerosol versus precipitation residue composition per sampling time period during CalWater 2010. Percentages represent either the number of each type of aerosol or residue per total number of aerosols or residues analyzed per sample. Sea salt was not observed in precipitation and biological particles were not observed in the ambient data.

was not observed in the precipitation due to its soluble nature, while biological particles were not observed as ambient aerosols likely due to the fact that the majority of these particles originated from soil dust and were separated during the resuspension process (Creamean et al., 2013, 2014a). For all three sampling seasons, the time periods with the highest relative amount of dust, biomass burning, or pollution residues in the precipitation samples did not correspond to the highest relative amount of the same type of ambient aerosol (i.e., almost all of the Spearman’s correlation coefficients ( $\rho$ ) were low or negative and did not demonstrate statistical significance as shown in Table 2). Herein, we employ the use of  $\rho$  to show the monotonic relationships between the residue composition and ambient aerosol or cloud and precipitation properties, since the relationship between aerosols and precipitation is not a linear function of two variables and other factors play a role. The absence of correlation between similar types of ambient aerosol versus precipitation residue particles may suggest that the majority of the residues were from nucleation of cloud particles, with a possible smaller contribution from scavenging during precipitation particle descent.

### 3.2 Linking residue composition to precipitation type and quantity using ATOFMS and S-PROF

As observed by Ault et al. (2011), aerosols can produce up to 40 % more precipitation during storms in the Sierra Nevada. Fan et al. (2014) showed the large impact that dust and biological aerosols can have on Sierra Nevada snowpack, where they simulated these aerosols increasing snowpack by 40 %. Further, Martin et al. (2015) simulated storms during CalWater in 2011 and demonstrated how the storms with more

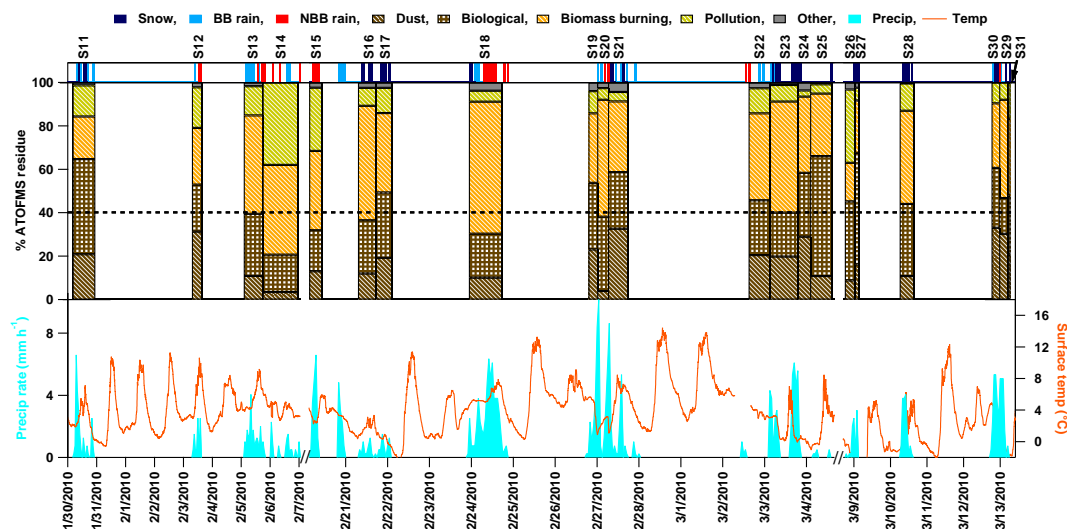


**Figure 3.** Precipitation process type (30 min), residue type (per sample), precipitation accumulation (1 h), and surface temperature (2 min) during all storms from 2010. Time periods without precipitation process measurements correspond to no falling precipitation or missing S-PROF data. Each precipitation sample bar of the residue types represents one sample and the width of the bar reflects the sample collection time period. Sample IDs are provided above each sample bar and correspond to those in Table 1. Note that the sample length is only shown during rain or snow and thus may not directly correspond to times provided in Table 1. The horizontal black dashed line represents the 40 % mark for ATOFMS.

**Table 2.** Spearman's correlation coefficients  $P$  values, and statistical significance of relationships between similar particle types that were found in the precipitation samples and ambient aerosols during the same time period of precipitation collection.

Year	Spearman	$P$	Significant
Dust			
2009	−0.43	0.21	No
2010	0.25	0.49	No
2011	0.58	0.08	No
Biomass burning			
2009	0.07	0.78	No
2010	0.21	0.40	No
2011	0.56	0.02	Yes
Pollution			
2009	0.08	0.83	No
2010	−0.08	0.83	No
2011	0.04	0.19	No

dust and biological particles incorporated into upper cloud levels produced 23 % (but as much as 67 %) more precipitation than storms with a greater influence from regional pollution aerosols. Variations in meteorological forcing also play a role in the precipitation type and quantity (Martin et al., 2015), but the rather systematic correlations between different aerosol sources and precipitation processes previously

shown and described herein suggest the aerosol sources can still play a vital role.

### 3.2.1 Dust and biological residues were dominant when precipitation formed as ice

Here, we demonstrate how the variability in the different sources of insoluble residues from aerosols influence both the type and quantity of precipitation during the CalWater storms in the Sierra Nevada. In most cases, the sources of the ATOFMS residues were correlated with the precipitation process type as delineated by the meteorological (S-PROF radar) measurements. This is demonstrated by the 2010 samples in Fig. 3 (2009 and 2011 are shown in Ault et al., 2011, and Creamean et al., 2013, respectively, but follow similar trends to the 2010 samples). Overall, BB rain or snow events (when surface temperatures dropped to  $\sim 0^\circ\text{C}$ ) were typically detected during time periods when precipitation samples contained higher percentages of dust plus biological residues (hereafter referred to as % Dust + Bio), particularly when Dust + Bio was  $>40\%$  of the total residues. Throughout this discussion, the dust and biological residues are combined to simulate the percentage of residue types that likely served as IN and because they are likely from a similar source (Creamean et al., 2013). However they are shown separately in the figures to demonstrate the relative contribution of each, which is particularly important for the biological residues as discussed in more detail below. Sample time periods with the most biomass burning and pollution residues typically corresponded to the most NBB rain dur-

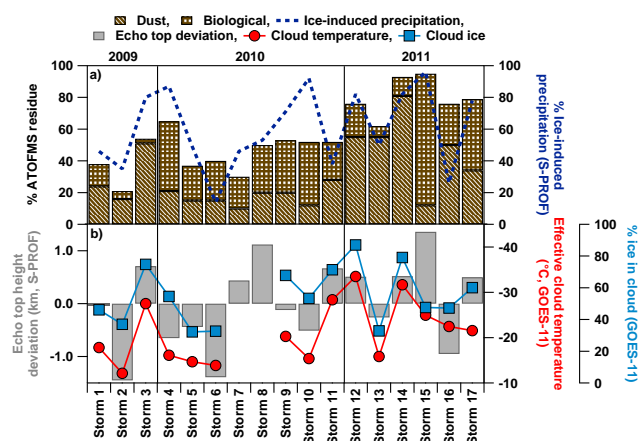


**Figure 4.** Summary of IN precipitation residue composition, observed surface meteorology at SPD, and cloud properties above SPD. (a) The percentages of dust and biological residues and the % ice-induced precipitation (snow plus BB rain). (b) Echo top height deviation (km) calculated from all storms during CalWater (average: 3.51 km based on data from 43 days during ATOFMS sample collection time periods provided in Table 1). Positive (negative) deviations correspond to higher (lower) than average echo top heights. Effective cloud temperature and percentage of cloud ice are also shown. Data were removed if in the homogeneous nucleation regime ( $\leq -36^\circ\text{C}$ ). The respective instruments in which each measurement was acquired is provided in the axis labels.

ing 2010, suggesting precipitation was formed as liquid due to the lesser influence from Dust + Bio. For instance, storm 5 in 2010 corresponded to samples with some of the lowest percentages of Dust + Bio (down to 20 %) and frequent detection of NBB rain (5 out of 13.5 h), particularly towards the end of the storm. BB rain was detected during the precipitation sampling at the end of this storm as well, possibly because Dust + Bio residues were still present and thus ice was still nucleated in the clouds above SPD. The sample from storm 7 (S18) also contained low % Dust + Bio (30 %), and frequent detection of NBB rain (6.5 out of 15 h). Overall, these results show that dust and biological residues were dominant during time periods when precipitation formed in the ice phase based on ATOFMS and S-PROF measurements.

Although 2010 samples contained very different relative contributions of residue types when compared to 2009 and 2011, the different residue types followed very similar relationships with cloud ice amounts, precipitation type and quantity, and cloud depth. Figures 4 and 5 provide a summary of observed meteorological conditions during each of the three winter sampling seasons in addition to precipitation residue composition averaged per storm and properties of clouds above SPD. Snow and BB rain are combined and denoted as “ice-induced precipitation”, i.e., precipitation that was initially formed as ice (Creamean et al., 2013). The echo top heights and storm-total precipitation are shown as deviations from their averages during all of CalWater storms

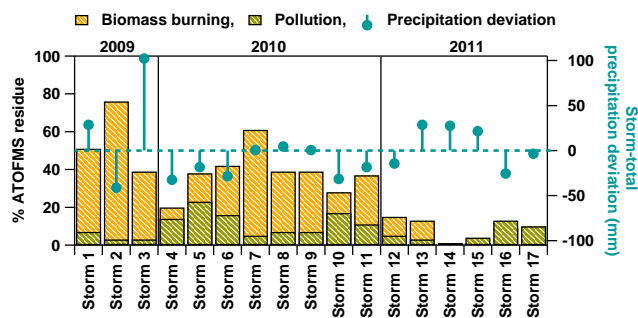


**Figure 5.** Summary of organic carbon precipitation residue composition and storm-total precipitation deviation. Organic carbon residues are separated into those from biomass burning and those from local pollution. Storm-total precipitation deviation (mm) is calculated from all storms during CalWater (average: 55.46 mm based on data from 43 days during ATOFMS sample collection time periods provided in Table 1). Positive (negative) deviations correspond to higher (lower) than average echo top heights.

to demonstrate the range of their variations: the echo top height average and storm-total precipitation averages were 3.51 km and 55.46 mm, respectively, based on data from 43 days during sample collection time periods provided in Table 1. Data from GOES-11 were removed if the cloud effective temperature was within the homogeneous nucleation regime ( $\leq -36^\circ\text{C}$ ; during storms 7 and 8) to enable the investigation of heterogeneous ice nucleation processes only. It is important to note that correlations are not statistically significant due to the low number (17) of events; however, they still provide a useful context to the trends between the residue composition and cloud and precipitation properties. As shown in Fig. 4, events with more ice-induced precipitation and cloud ice typically correspond to samples with more dust and/or biological residues ( $\rho = 0.58$  and  $0.67$ , respectively, for Dust + Bio). Correlation plots and Spearman’s correlation coefficients for Dust + Bio versus ice-induced precipitation and cloud ice are shown in the Supplement figure S1, along with correlation plots for Dust + Bio versus echo top height deviation. This relationship supports our hypothesis that the majority of the residues were nucleated as opposed to scavenged. If, for example, most of the residues were scavenged, we might not expect such strong relationships of dust and biological residues with the amount of cloud ice and ice-induced precipitation.

In particular, the storms with the highest Dust + Bio (storms 14 and 15; 93 and 95 %, respectively) correspond to some of the highest values of ice-induced precipitation (82 and 96 %, respectively). Interestingly, these two storms had very different residue composition: storm 14 had more dust (81 %), whereas storm 15 had more biological residues (83 %). The effective cloud temperatures were  $-32$  and  $-25^\circ\text{C}$ , respectively, suggesting that the dust IN were more effective at colder temperatures, while the biological IN were active at warmer temperatures. Other interesting cases are

storms 4 and 10 from 2010, where biological residues composed 80 and 77 % of the potential IN and ice-induced precipitation was 87 and 92 %, respectively. Cloud temperatures were also relatively warm during these storms ( $-16$  and  $-15$  °C, respectively), further demonstrating that biological IN are active at warmer temperatures. In the cases where biological residues were dominant during storms 3, 10, and 15 and likely served as IN at warmer cloud temperatures, the cloud ice content was  $\geq 50$  % based on GOES-11 measurements. It is important to note that the purely biological residues could be a result of the aerosolization process and thus might have originally been components of the dust particles. Although biological particles were not observed as ambient aerosol at the ground, they were observed as interstitial aerosol and in individual cloud particles during the 2011 in-cloud aircraft measurements (Creamean et al., 2013). The likelihood that the majority of the biological residues are separated from the dust during the aerosolization process is supported by the following: (1) a higher abundance of purely biological residues was observed in the precipitation samples compared to the interstitial aerosol or cloud particles and (2) a higher abundance of dust mixed with biological material was observed in the aircraft measurements compared to the precipitation collected on the ground. Even considering this issue, the dust particles that were present in cloud still contained more biological material during time periods with warmer cloud temperatures and thus would have enabled the dust to serve as more efficient IN as delineated by Conen et al. (2011) and O'Sullivan et al. (2014).

The percentages of dust and biological residues were also generally in phase with the echo top height deviation as shown in Fig. 4 ( $\rho = 0.39$ ): when the clouds were deeper, i.e., larger positive echo top height deviation (shallower, i.e., larger negative echo top height deviation), the % Dust + Bio was higher (lower) as was the relative amount of ice-induced precipitation. However, storm 10 was atypical; the % ice-induced precipitation was high (92 %), while % Dust + Bio was not as high (52 %), which could be a result of the clouds being shallower. Based on these results, we suggest that when the clouds were sufficiently deep, they were more likely to have incorporated long-range-transported dust and biological aerosols that were present only at higher altitudes (above  $\sim 3$  km), such as in the cases documented by Ault et al. (2011) and Creamean et al. (2013), and the simulations of storms 13 and 14 by Martin et al. (2015). These dust and biological aerosols likely initiated ice formation and thus influenced the relative amount of ice-induced precipitation.

### 3.2.2 Shallow clouds associated with aerosols from local biomass burning and pollution produced less precipitation

In contrast, when clouds were more shallow, (1) dust and biological aerosols likely traveled over the cloud tops, and thus did not become incorporated, and/or (2) less dust and

biological aerosols were transported into the region. Thus a larger influence from local aerosols in the form of biomass burning and pollution residues was observed, as shown in Fig. 5. Local biomass burning residues composed most of the OC residues (78 %) compared to pollution (22 %), particularly in 2009 and 2010. On average, biomass burning (31 %) and pollution residues (9 %) did not constitute as many of the residues as Dust + Bio (55 %). Figure 5 also shows the relationship between OC residues (biomass burning and pollution) and storm-total precipitation deviation. Generally, events with a negative storm-total precipitation deviation corresponded to precipitation samples containing more OC residues ( $\rho = -0.38$ ), i.e., the combined percentage of biomass burning and pollution residues was out of phase with the storm-total precipitation deviation. For instance, the highest percentage of OC residue types (storm 2) had the largest negative storm-total precipitation deviation. Correlation plots and Spearman's correlation coefficients for OC versus precipitation deviation are shown in the Fig. S1. Further, storms 13–15 in 2011 had some of the lowest percentages of OC residues and some of the largest positive storm-total precipitation deviations compared to the remaining 2011 storms. The OC residues from local biomass burning and pollution likely served as CCN and seeded the lower levels of orographic clouds, resulting in smaller cloud droplets that are less efficiently scavenged during the riming process (Borys et al., 2000; Rosenfeld and Givati, 2006; Saleeby et al., 2009).

Although CCN are typically thought to be soluble in nature, partially soluble or insoluble organic-containing aerosols have been shown to serve as CCN as well. For instance, CCN closure studies have found better agreement between predicted and observed CCN concentrations when insoluble organic particles were used in their simulations (Broekhuizen et al., 2006; Wang et al., 2008; Ervens et al., 2010). Further, previous studies have shown that relatively insoluble organic particles with small amounts of soluble inorganic material, such as sodium chloride, can drive the CCN activity of the organic particles (Broekhuizen et al., 2004; Ervens et al., 2010). Even partially or slightly soluble organics have been shown to serve as CCN (Bilde and Svenningsson, 2004), particularly if the particles were wet instead of dry (Henning et al., 2005). For the 2009 samples, measurements of select soluble species were acquired and presented by Creamean et al. (2014a). Results presented there showed correlations between sodium, potassium, sulfate, chloride, nitrate, and phosphate and insoluble OC residues, thus signifying that these insoluble OC residues were likely cores of the original particles from biomass burning and/or pollution. Therefore, the OC residues observed in all the CalWater samples, although insoluble, could have potentially originated as cores with soluble species on the surfaces or partially soluble organic particles that remained intact while in solution, enabling them to serve as CCN and lead to the relationships with shallow clouds and negative precipitation deviation.

#### 4 Broader implications

Overall, the results from this study demonstrate the interannual variability in the sources of aerosols seeding clouds over the Sierra Nevada as indicated by the insoluble residue composition. The combination of dust and biological residues, aerosols that likely served as IN, increased over time from 2009 to 2011, whereas the organic carbon residues (including local biomass burning and pollution residues) decreased over time. Further, the level at which the cloud nuclei impact cloud formation is important for resulting effects on precipitation processes: dust and biological residues likely serve as IN at higher altitudes in cloud, while organic carbon residues serve as CCN at cloud base. However, this study presents a limited number of data points and thus needs to be extended by future, additional measurements. It has been shown that dust and biological aerosols originate from long-range transport to the Sierra Nevada, whereas biomass burning and pollution residues are more likely from local sources (Rosenfeld and Givati, 2006; Ault et al., 2011; Creamean et al., 2013). Dust and biological residues were ubiquitous in the most of the samples, which induced the formation of ice precipitation, particularly corresponding to time periods when the samples contained a relatively high amount of biological residues. This suggests the residues containing biological material served as more efficient IN than dust. The two storms with the highest percentages of either dust (storm 14) or biological (storm 15) residues demonstrate this effect, where storm 15 produced more ice-induced precipitation and had higher cloud temperatures, whereas much lower cloud temperatures were observed during storm 14. Sample 35 (S35 from storm 14) contained mainly mineral dust with little to no biological material as shown from IN measurements and heat treatment of the sample by Creamean et al. (2014a). Creamean et al. (2014a) also conducted the same measurements on the sample from storm 15 (S38), which contained IN active at high temperatures. Thus, the comparison of the samples from storms 14 and 15 enables us to determine the IN efficiency of dust versus biological material, both from previous laboratory measurements and in situ observations. Storms 4 and 10 contained more biological residues and produced substantial amounts of precipitation formed as ice under high cloud temperatures, further corroborating the fact that biological aerosols are more effective IN.

The source of the insoluble residues influenced whether precipitation formed in the ice or liquid phase, and also likely affected the quantity of precipitation that fell at SPD. Larger quantities of precipitation in comparison to the average from all three sampling seasons were observed during time periods when dust and biological residues were predominant in the samples. The most plausible explanation for this, as described previously, is that these residues likely served as IN which led to efficient riming processes and enhanced precipitation formation (Ault et al., 2011; Creamean et al., 2013, 2014a). In contrast, OC residues from both biomass burn-

ing and to some extent pollution were observed during time periods with less precipitation. One possibility is that the local biomass burning and pollution residues served as CCN, which enhanced cloud droplet formation after being incorporated into lower levels of the orographic clouds and led to less precipitation (Weaver et al., 2002; Rosenfeld and Givati, 2006; Rosenfeld et al., 2008; Saleeby et al., 2009). A modeling study of aircraft measurements from 2011 presented by Martin et al. (2015) shows the presence of organic carbon residues at lower cloud levels during prefrontal storm conditions in the Sierra Nevada, demonstrating the significance of our observations and how they validate model results. The cloud droplets formed from biomass burning and pollution likely decreased the riming efficiency of the ice crystals formed at higher altitudes in the presence of dust and biological aerosols, subsequently contributing to time periods with less ice-induced precipitation. With fewer aerosol seeds, cloud droplets and ice crystals form much less frequently under typical atmospheric conditions in the lower troposphere over the Sierra Nevada, altering the quantity of precipitation. Previous studies have shown that aerosols can have a significant impact on precipitation quantity and type in the Sierra Nevada during strong winter storms (Ault et al., 2011; Creamean et al., 2013; Fan et al., 2014; Martin et al., 2015). Based on this, the results presented here are in agreement with previous research.

Fan et al. (2014) and Martin et al. (2015) demonstrate the reproducibility of the observations in the Weather Research and Forecasting (WRF) model by focusing on particular case studies from CalWater 2011. Observations presented herein for all CalWater storms will be incorporated into future modeling work to improve simulations. However, future work is needed to better isolate the impacts of storm dynamics, aerosol microphysics, and precipitation, particularly when incorporating observations into regional climate models. Ultimately, the goal is to develop a mechanistic understanding of how, when, and where different aerosol sources influence cloud microphysics and the resulting precipitation in the Sierra Nevada. Improvement of these models can be used as predictive tools for future weather forecasts.

#### 5 Conclusions

Observed variations of sources of the insoluble residues from aerosols serving as CCN and IN in Sierra Nevada precipitation were documented during three winter sampling seasons as part of the CalWater field program. These variations were then compared with meteorological observations of precipitation characteristics aloft during the same events. Insoluble residues in precipitation samples were used to link aerosol sources with trends in precipitation characteristics. The unique multi-year, multi-event, and co-located aerosol and meteorological observations enabled the development of the following main conclusions:

- Differences in aerosol sources seeding the clouds based on the composition of insoluble residues were observed from year to year and between storms. We present cases with predominantly long-range-transported dust and biological residues (2011), local biomass burning and pollution residues (2010), or a combination of these sources (2009).
- Although the residues in the 2010 samples were vastly different (i.e., influenced more by biomass burning), the relationships between the dust and biological residues and cloud ice, precipitation type and quantity, and cloud depth were consistent with 2009 and 2011 samples.
- Dust and biological residues serve as IN, becoming incorporated into deeper cloud systems at cloud top and subsequently influencing the formation of ice-induced precipitation at SPD. This effect was documented in the CalWater 2011 modeling study by Fan et al. (2014).
- Our observations support the hypothesis that biomass burning and pollution residues likely served as CCN in shallower orographic clouds, which coincided with periods of less precipitation as simulated by Martin et al. (2015) during two CalWater 2011 storms in the Sierra Nevada.
- When dust/biological residues and pollution/biomass burning residues were both present, orographic clouds also were typically shallow and coincided with periods of less precipitation. This aligns with the hypothesis that IN and high concentrations of CCN at different altitudes in the same cloud system inhibit precipitation formation (Saleeby et al., 2009).

By building on previous case studies presented by Ault et al. (2011) and Creamean et al. (2013), results presented herein represent a noteworthy advancement in understanding the effects of sources of insoluble aerosol species on the type and quantity of precipitation in the California Sierra Nevada. Aerosol impacts on clouds and precipitation derived from insoluble residue links with cloud and precipitation properties have important implications for the Sierra Nevada by serving as one of the key factors that influence water supply in the region. The relationships between insoluble precipitation residues and their potential climate impacts could translate to a global scale, i.e., apply to other orographic regions where such insoluble particles are found in and impact the formation of clouds and precipitation. Thus, understanding insoluble residue sources has implications on a global level, particularly when modeling their impacts on clouds. However, additional studies are needed to better quantify these relationships, which served as a major motivation for the more recent CalWater 2 field campaign, which started in early 2015. The findings presented here from CalWater served as the foundation for the flight planning and execution of field measurements during CalWater 2, demonstrating

the importance of our results for not only constraining future modeling work but also serving as a driver to continue similar measurements to develop a longer-term record. Results from both studies will enable improvements in models to better assess how weather patterns and/or regional climate may change due to the effects from different aerosol sources, particularly those from long-range transport which have a major impact on the seeder–feeder mechanism long observed over the Sierra Nevada. Improving our ability to model the interactions between aerosols, clouds, and precipitation can contribute to better winter storm preparedness, water resource management, and flood mitigation.

**The Supplement related to this article is available online at doi:10.5194/acp-15-6535-2015-supplement.**

*Author contributions.* J. M. Creamean collected and analyzed ATOFMS data from precipitation samples in 2009, 2010, and 2011, interpreted all data, and prepared the manuscript with contributions from all co-authors. A. P. Ault collected and analyzed ATOFMS data from precipitation samples in 2009. A. B. White, P. J. Neiman, and F. M. Ralph collected and analyzed S-PROF data and surface meteorology measurements at SPD. P. Minnis analyzed GOES-11 data. F. M. Ralph was additionally involved with experimental design. K. A. Prather was the principal investigator of this study, involved with experimental design as well as preparation and editing of this manuscript. All authors reviewed and commented on the paper.

*Acknowledgements.* Surface meteorological measurements and S-PROF radar data were retrieved from NOAA HMT-West (<http://hmt.noaa.gov/>). Funding was provided by the California Energy Commission under contract UCOP/CIEE C-09-07 and CEC 500-09-043. J. Creamean was partially supported by the National Research Council Research Associateship Program. P. Minnis was supported by the NASA Modeling, Analysis, and Prediction Program and the DOE ARM Program. J. Mayer, D. Collins, J. Cahill, M. Zauscher, E. Fitzgerald, C. Gaston, and M. Moore from UCSD provided assistance with equipment preparation and setup at SPD. The deployment of the NOAA and UCSD/SIO equipment at SPD involved many field staff, particularly C. King (NOAA). The Forest Hill Power Utility District is acknowledged for hosting the sampling site at SPD. A. Martin (UCSD), G. Wick (NOAA), and D. Gottas (NOAA) provided insightful discussions.

Edited by: A. Huffman

## References

- Allen, J. O.: Quantitative Analysis of Aerosol Time-of-Flight Mass Spectrometry Data using YAADA, Arizona State University, Tempe, Arizona, USA, 2004.
- Ault, A. P., Williams, C. R., White, A. B., Neiman, P. J., Creamean, J. M., Gaston, C. J., Ralph, F. M., and Prather, K. A.: Detection of Asian dust in California orographic precipitation, *J. Geophys. Res.-Atmos.*, 116, doi:10.1029/2010JD015351, 2011.
- Bergeron, T.: On the physics of cloud and precipitation, in: 5th Assembly of the U. G. G. I., Paul Dupont, Paris, 1935.
- Bilde, M. and Svenningsson, B.: CCN activation of slightly soluble organics: the importance of small amounts of inorganic salt and particle phase, *Tellus B*, 56, 128–134, doi:10.1111/j.1600-0889.2004.00090.x, 2004.
- Borys, R. D., Lowenthal, D. H., and Mitchell, D. L.: The relationships among cloud microphysics, chemistry, and precipitation rate in cold mountain clouds, *Atmos. Environ.*, 34, 2593–2602, 2000.
- Broekhuizen, K., Kumar, P. P., and Abbatt, J. P. D.: Partially soluble organics as cloud condensation nuclei: Role of trace soluble and surface active species, *Geophys. Res. Lett.*, 31, L01107, doi:10.1029/2003gl018203, 2004.
- Broekhuizen, K., Chang, R.Y.-W., Leaitch, W. R., Li, S.-M., and Abbatt, J. P. D.: Closure between measured and modeled cloud condensation nuclei (CCN) using size-resolved aerosol compositions in downtown Toronto, *Atmos. Chem. Phys.*, 6, 2513–2524, doi:10.5194/acp-6-2513-2006, 2006.
- Carrico, C. M., Petters, M. D., Kreidenweis, S. M., Sullivan, A. P., McMeeking, G. R., Levin, E. J. T., Engling, G., Malm, W. C., and Collett Jr., J. L.: Water uptake and chemical composition of fresh aerosols generated in open burning of biomass, *Atmos. Chem. Phys.*, 10, 5165–5178, doi:10.5194/acp-10-5165-2010, 2010.
- Choulaton, T. W. and Perry, S. J.: A model of the orographic enhancement of snowfall by the seeder–feeder mechanism, *Q. J. Roy. Meteor. Soc.*, 112, 335–345, 1986.
- Colle, B. A. and Zeng, Y. G.: Bulk microphysical sensitivities within the MM5 for orographic precipitation. Part I: The Sierra 1986 event, *Mon. Weather Rev.*, 132, 2780–2801, 2004.
- Collett, J. L., Daube, B. C., Gunz, D., and Hoffmann, M. R.: Intensive studies of Sierra-Nevada cloudwater chemistry and its relationship to precursor aerosol and gas concentrations, *Atmos. Environ. A-Gen.*, 24, 1741–1757, 1990.
- Conen, F., Morris, C. E., Leifeld, J., Yakutin, M. V., and Alewell, C.: Biological residues define the ice nucleation properties of soil dust, *Atmos. Chem. Phys.*, 11, 9643–9648, doi:10.5194/acp-11-9643-2011, 2011.
- Creamean, J. M., Ault, A. P., Ten Hoeve, J. E., Jacobson, M. Z., Roberts, G. C., and Prather, K. A.: Measurements of aerosol chemistry during new particle formation events at a remote rural mountain site, *Environ. Sci. Technol.*, 45, 8208–8216, doi:10.1021/Es103692f, 2011.
- Creamean, J. M., Suski, K. J., Rosenfeld, D., Cazorla, A., DeMott, P. J., Sullivan, R. C., White, A. B., Ralph, F. M., Minnis, P., Comstock, J. M., Tomlinson, J. M., and Prather, K. A.: Dust and biological aerosols from the Sahara and Asia influence precipitation in the western US, *Science*, 339, 1572–1578, 2013.
- Creamean, J. M., Lee, C., Hill, T. C., Ault, A. P., DeMott, P. J., White, A. B., Ralph, F. M., and Prather, K. A.: Chemical properties of insoluble precipitation residue particles, *J. Aerosol Sci.*, 76, 13–27, 2014a.
- Creamean, J. M., Spackman, J. R., Davis, S. M., and White, A. B.: Climatology of long-range transported Asian dust on the west coast of the United States, *J. Geophys. Res.-Atmos.*, 119, 12171–12185, 2014b.
- DeMott, P. J., Sassen, K., Poellot, M. R., Baumgardner, D., Rogers, D. C., Brooks, S. D., Prenni, A. J., and Kreidenweis, S. M.: African dust aerosols as atmospheric ice nuclei, *Geophys. Res. Lett.*, 30, 1732, doi:10.1029/2003gl017410, 2003.
- Deshler, T. and Reynolds, D. W.: Physical response of winter orographic clouds over the Sierra-Nevada to airborne seeding using dry ice or silver-iodide, *J. Appl. Meteorol.*, 29, 288–330, 1990.
- Despres, V. R., Huffman, J. A., Burrows, S. M., Hoose, C., Safatov, A. S., Buryak, G., Frohlich-Nowoisky, J., Elbert, W., Andreae, M. O., Pöschl, U., and Jaenicke, R.: Primary biological aerosol particles in the atmosphere: a review, *Tellus B*, 64, doi:10.3402/tellusb.v64i0.15598, 2012.
- Dettinger, M., Ralph, F. M., Das, T., Neiman, P. J., and Cayan, D. R.: Atmospheric rivers, floods and the water resources of California, *Water*, 3, 445–478, doi:10.3390/w3020445, 2011.
- Engelhart, G. J., Hennigan, C. J., Miracolo, M. A., Robinson, A. L., and Pandis, S. N.: Cloud condensation nuclei activity of fresh primary and aged biomass burning aerosol, *Atmos. Chem. Phys.*, 12, 7285–7293, doi:10.5194/acp-12-7285-2012, 2012.
- Ervens, B., Cubison, M. J., Andrews, E., Feingold, G., Ogren, J. A., Jimenez, J. L., Quinn, P. K., Bates, T. S., Wang, J., Zhang, Q., Coe, H., Flynn, M., and Allan, J. D.: CCN predictions using simplified assumptions of organic aerosol composition and mixing state: a synthesis from six different locations, *Atmos. Chem. Phys.*, 10, 4795–4807, doi:10.5194/acp-10-4795-2010, 2010.
- Fan, J., Leung, L. R., DeMott, P. J., Comstock, J. M., Singh, B., Rosenfeld, D., Tomlinson, J. M., White, A., Prather, K. A., Minnis, P., Ayers, J. K., and Min, Q.: Aerosol impacts on California winter clouds and precipitation during CalWater 2011: local pollution versus long-range transported dust, *Atmos. Chem. Phys.*, 14, 81–101, doi:10.5194/acp-14-81-2014, 2014.
- Field, P. R., Möhler, O., Connolly, P., Krämer, M., Cotton, R., Heymsfield, A. J., Saathoff, H., and Schnaiter, M.: Some ice nucleation characteristics of Asian and Saharan desert dust, *Atmos. Chem. Phys.*, 6, 2991–3006, doi:10.5194/acp-6-2991-2006, 2006.
- Gard, E., Mayer, J. E., Morrical, B. D., Dienes, T., Fergenson, D. P., and Prather, K. A.: Real-time analysis of individual atmospheric aerosol particles: design and performance of a portable ATOFMS, *Anal. Chem.*, 69, 4083–4091, 1997.
- Gaston, C. J., Quinn, P. K., Bates, T. S., Gilman, J. B., Bon, D. M., Kuster, W. C., and Prather, K. A.: The impact of shipping, agricultural, and urban emissions on single particle chemistry observed aboard the R/V *Atlantis* during CalNex, *J. Geophys. Res.-Atmos.*, 118, 5003–5017, doi:10.1002/Jgrd.50427, 2013.
- Givati, A. and Rosenfeld, D.: Quantifying precipitation suppression due to air pollution, *J. Appl. Meteorol.*, 43, 1038–1056, 2004.
- Guan, B., Molotch, N. P., Waliser, D. E., Fetzer, E. J., and Neiman, P. J.: Extreme snowfall events linked to atmospheric rivers and surface air temperature via satellite measurements, *Geophys. Res. Lett.*, 37, L20401, doi:10.1029/2010gl044696, 2010.

- Henning, S., Rosenørn, T., D'Anna, B., Gola, A. A., Svenningsson, B., and Bilde, M.: Cloud droplet activation and surface tension of mixtures of slightly soluble organics and inorganic salt, *Atmos. Chem. Phys.*, 5, 575–582, doi:10.5194/acp-5-575-2005, 2005.
- Holecek, J. C., Spencer, M. T., and Prather, K. A.: Analysis of rainwater samples: comparison of single particle residues with ambient particle chemistry from the northeast Pacific and Indian oceans, *J. Geophys. Res.-Atmos.*, 112, D22s24, doi:10.1029/2006jd008269, 2007.
- Hosler, C. L., Jensen, D. C., and Goldshlak, L.: On the aggregation of ice crystals to form snow, *J. Meteorol.*, 14, 415–420, 1957.
- Husar, R. B., Tratt, D. M., Schichtel, B. A., Falke, S. R., Li, F., Jaffe, D., Gasso, S., Gill, T., Laulainen, N. S., Lu, F., Reheis, M. C., Chun, Y., Westphal, D., Holben, B. N., Gueymard, C., McKendry, I., Kuring, N., Feldman, G. C., McClain, C., Frouin, R. J., Merrill, J., DuBois, D., Vignola, F., Murayama, T., Nickovic, S., Wilson, W. E., Sassen, K., Sugimoto, N., and Malm, W. C.: Asian dust events of April 1998, *J. Geophys. Res.-Atmos.*, 106, 18317–18330, doi:10.1029/2000jd900788, 2001.
- Jaffe, D., Tamura, S., and Harris, J.: Seasonal cycle and composition of background fine particles along the west coast of the US, *Atmos. Environ.*, 39, 297–306, doi:10.1016/j.atmosenv.2004.09.016, 2005.
- Liu, W., Hopke, P. K., and VanCuren, R. A.: Origins of fine aerosol mass in the western United States using positive matrix factorization, *J. Geophys. Res.-Atmos.*, 108, 4716, doi:10.1029/2003jd003678, 2003.
- Lunden, M. M., Black, D. R., McKay, M., Revzan, K. L., Goldstein, A. H., and Brown, N. J.: Characteristics of fine particle growth events observed above a forested ecosystem in the Sierra Nevada Mountains of California, *Aerosol Sci. Tech.*, 40, 373–388, 2006.
- Marcolli, C., Gedamke, S., Peter, T., and Zobrist, B.: Efficiency of immersion mode ice nucleation on surrogates of mineral dust, *Atmos. Chem. Phys.*, 7, 5081–5091, doi:10.5194/acp-7-5081-2007, 2007.
- Martin, A., Prather, K. A., Leung, L. R., and Suski, K. J.: Simulated intra-storm variability in aerosol driven precipitation enhancement during US West Coast winter storms, *J. Aerosol Sci.*, in review, 2015.
- Martner, B. E., Yuter, S. E., White, A. B., Matrosov, S. Y., Kingsmill, D. E., and Ralph, F. M.: Raindrop size distributions and rain characteristics in California coastal rainfall for periods with and without a radar bright band, *J. Hydrometeorol.*, 9, 408–425, doi:10.1175/2007jhm924.1, 2008.
- McGregor, K. G. and Anastasio, C.: Chemistry of fog waters in California's Central Valley: 2. Photochemical transformations of amino acids and alkyl amines, *Atmos. Environ.*, 35, 1091–1104, doi:10.1016/S1352-2310(00)00282-X, 2001.
- McKendry, I. G., Strawbridge, K. B., O'Neill, N. T., Macdonald, A. M., Liu, P. S. K., Leitch, W. R., Anlauf, K. G., Jaegle, L., Fairlie, T. D., and Westphal, D. L.: Trans-Pacific transport of Saharan dust to western North America: a case study, *J. Geophys. Res.-Atmos.*, 112, D01103, doi:10.1029/2006jd007129, 2007.
- Meyers, M. P., Demott, P. J., and Cotton, W. R.: New primary ice-nucleation parameterizations in an explicit cloud model, *J. Appl. Meteorol.*, 31, 708–721, 1992.
- Minnis, P., Nguyen, L., Palikonda, R., Heck, P. W., Spangenberg, D. A., Doelling, D. R., Ayers, J. K., Smith, W. L., Khaiyer, M. M., Trepte, Q. Z., Avey, L. A., Chang, F.-L., Yost, C. R., Chee, T. L., and Sun-Mack, S.: Near-real time cloud retrievals from operational and research meteorological satellites, in: *Proc. SPIE Europe Remote Sens.*, Cardiff, Wales, UK, 15–18 September 2008, 2008.
- Minnis, P., Sun-Mack, S., Young, D. F., Heck, P. W., Garber, D. P., Chen, Y., Spangenberg, D. A., Arduini, R. F., Trepte, Q. Z., Jr., W. L., Spangenberg, D. A., Ayers, J. K., Gibson, S. C., Miller, W. F., Chakrapani, V., Takano, Y., Liou, K.-N., Xie, Y., and Yang, P.: CERES Edition-2 cloud property retrievals using TRMM VIRS and Terra and Aqua MODIS data, Part I: Algorithms, *IEEE T. Geosci. Remote*, 49, doi:10.1109/TGRS.2011.2144601, 2011.
- Morris, C. E., Georgakopoulos, D. G., and Sands, D. C.: Ice nucleation active bacteria and their potential role in precipitation, *J. Phys. Iv.*, 121, 87–103, doi:10.1051/jp4:2004121004, 2004.
- Muhlbauer, A., Hashino, T., Xue, L., Teller, A., Lohmann, U., Rasmussen, R. M., Geresdi, I., and Pan, Z.: Intercomparison of aerosol-cloud-precipitation interactions in stratiform orographic mixed-phase clouds, *Atmos. Chem. Phys.*, 10, 8173–8196, doi:10.5194/acp-10-8173-2010, 2010.
- Murray, B. J., O'Sullivan, D., Atkinson, J. D., and Webb, M. E.: Ice nucleation by particles immersed in supercooled cloud droplets, *Chem. Soc. Rev.*, 41, 6519–6554, doi:10.1039/C2cs35200a, 2012.
- Neiman, P. J., Wick, G. A., Ralph, F. M., Martner, B. E., White, A. B., and Kingsmill, D. E.: Wintertime nonbrightband rain in California and Oregon during CALJET and PACJET: geographic, interannual, and synoptic variability, *Mon. Weather Rev.*, 133, 1199–1223, doi:10.1175/Mwr2919.1, 2005.
- O'Sullivan, D., Murray, B. J., Malkin, T. L., Whale, T. F., Umo, N. S., Atkinson, J. D., Price, H. C., Baustian, K. J., Browse, J., and Webb, M. E.: Ice nucleation by fertile soil dusts: relative importance of mineral and biogenic components, *Atmos. Chem. Phys.*, 14, 1853–1867, doi:10.5194/acp-14-1853-2014, 2014.
- Pandey, G. R., Cayan, D. R., and Georgakakos, K. P.: Precipitation structure in the Sierra Nevada of California during winter, *J. Geophys. Res.-Atmos.*, 104, 12019–12030, 1999.
- Pinsky, M., Khain, A., Rosenfeld, D., and Pokrovsky, A.: Comparison of collision velocity differences of drops and graupel particles in a very turbulent cloud, *Atmos. Res.*, 49, 99–113, 1998.
- Prather, K. A., Bertram, T. H., Grassian, V. H., Deane, G. B., Stokes, M. D., DeMott, P. J., Aluwihare, L. I., Palenik, B. P., Azam, F., Seinfeld, J. H., Moffet, R. C., Molina, M. J., Cappa, C. D., Geiger, F. M., Roberts, G. C., Russell, L. M., Ault, A. P., Baltusaitis, J., Collins, D. B., Corrigan, C. E., Cuadra-Rodriguez, L. A., Ebben, C. J., Forestieri, S. D., Guasco, T. L., Hersey, S. P., Kim, M. J., Lambert, W. F., Modini, R. L., Mui, W., Pedler, B. E., Ruppel, M. J., Ryder, O. S., Schoepp, N. G., Sullivan, R. C., and Zhao, D. F.: Bringing the ocean into the laboratory to probe the chemical complexity of sea spray aerosol, *P. Natl. Acad. Sci. USA*, 110, 7550–7555, doi:10.1073/pnas.1300262110, 2013.
- Pratt, K. A., DeMott, P. J., French, J. R., Wang, Z., Westphal, D. L., Heymsfield, A. J., Twohy, C. H., Prenni, A. J., and Prather, K. A.: In situ detection of biological particles in cloud ice-crystals, *Nat. Geosci.*, 2, 397–400, doi:10.1038/Ngeo521, 2009.

- Ralph, F. M., Neiman, P. J., and Wick, G. A.: Satellite and CALJET aircraft observations of atmospheric rivers over the eastern north pacific ocean during the winter of 1997/98, *Mon. Weather Rev.*, 132, 1721–1745, 2004.
- Ralph, F. M., Coleman, T., Neiman, P. J., Zamora, R. J., and Dettinger, M.: Observed impacts of duration and seasonality of atmospheric-river landfalls on soil moisture and runoff in coastal northern California, *J. Hydrometeorol.*, 14, 443–459, 2013a.
- Ralph, F. M., Intrieri, J., Andra, D., Atlas, R., Boukabara, S., Bright, D., Davidson, P., Entwistle, B., Gaynor, J., Goodman, S., Jiing, J. G., Harless, A., Huang, J., Jedlovec, G., Kain, J., Koch, S., Kuo, B., Levit, J., Murillo, S., Riishojgaard, L. P., Schneider, T., Schneider, R., Smith, T., and Weiss, S.: The emergence of weather-related test beds linking research and forecasting operations, *B. Am. Meteorol. Soc.*, 94, 1187–1211, doi:10.1175/Bams-D-12-00080.1, 2013b.
- Reynolds, D. W. and Dennis, A. S.: A review of the sierra cooperative pilot project, *B. Am. Meteorol. Soc.*, 67, 513–523, doi:10.1175/1520-0477(1986)067<0513:arotsc>2.0.co;2, 1986.
- Rosenfeld, D.: Suppression of rain and snow by urban and industrial air pollution, *Science*, 287, 1793–1796, 2000.
- Rosenfeld, D. and Givati, A.: Evidence of orographic precipitation suppression by air pollution-induced aerosols in the western United States, *J. Appl. Meteorol. Clim.*, 45, 893–911, 2006.
- Rosenfeld, D., Lohmann, U., Raga, G. B., O'Dowd, C. D., Kulmala, M., Fuzzi, S., Reissell, A., and Andreae, M. O.: Flood or drought: how do aerosols affect precipitation?, *Science*, 321, 1309–1313, doi:10.1126/science.1160606, 2008.
- Saleeby, S. M., Cotton, W. R., Lowenthal, D., Borys, R. D., and Wetzel, M. A.: Influence of Cloud Condensation Nuclei on Orographic Snowfall, *J. Appl. Meteorol. Clim.*, 48, 903–922, 2009.
- Song, X. H., Hopke, P. K., Fergenson, D. P., and Prather, K. A.: Classification of single particles analyzed by ATOFMS using an artificial neural network, ART-2A, *Anal. Chem.*, 71, 860–865, 1999.
- Tobo, Y., Prenni, A. J., DeMott, P. J., Huffman, J. A., McCluskey, C. S., Tian, G. X., Pohlker, C., Poschl, U., and Kreidenweis, S. M.: Biological aerosol particles as a key determinant of ice nuclei populations in a forest ecosystem, *J. Geophys. Res.-Atmos.*, 118, 10100–10110, doi:10.1002/Jgrd.50801, 2013.
- Uno, I., Eguchi, K., Yumimoto, K., Liu, Z., Hara, Y., Sugimoto, N., Shimizu, A., and Takemura, T.: Large Asian dust layers continuously reached North America in April 2010, *Atmos. Chem. Phys.*, 11, 7333–7341, doi:10.5194/acp-11-7333-2011, 2011.
- VanCuren, R. A. and Cahill, T. A.: Asian aerosols in North America: Frequency and concentration of fine dust, *J. Geophys. Res.-Atmos.*, 107, 4804, doi:10.1029/2002jd002204, 2002.
- Wang, J., Lee, Y.-N., Daum, P. H., Jayne, J., and Alexander, M. L.: Effects of aerosol organics on cloud condensation nucleus (CCN) concentration and first indirect aerosol effect, *Atmos. Chem. Phys.*, 8, 6325–6339, doi:10.5194/acp-8-6325-2008, 2008.
- Warburton, J. A., Young, L. G., and Stone, R. H.: Assessment of seeding effects in snowpack augmentation programs – ice nucleation and scavenging of seeding aerosols, *J. Appl. Meteorol.*, 34, 121–130, 1995.
- Weaver, J. F., Knaff, J. A., Bikos, D., Wade, G. S., and Daniels, J. M.: Satellite observations of a severe supercell thunderstorm on 24 July 2000 made during the GOES-11 science test, *Weather Forecast*, 17, 124–138, 2002.
- White, A. B., Jordan, J. R., Martner, B. E., Ralph, F. M., and Bartram, B. W.: Extending the dynamic range of an S-band radar for cloud and precipitation studies, *J. Atmos. Ocean. Tech.*, 17, 1226–1234, doi:10.1175/1520-0426(2000)017<1226:Etdroa>2.0.Co;2, 2000.
- White, A. B., Gottas, D. J., Strem, E. T., Ralph, F. M., and Neiman, P. J.: An automated brightband height detection algorithm for use with Doppler radar spectral moments, *J. Atmos. Ocean. Tech.*, 19, 687–697, 2002.
- White, A. B., Neiman, P. J., Ralph, F. M., Kingsmill, D. E., and Persson, P. O. G.: Coastal orographic rainfall processes observed by radar during the California land-falling jets experiment, *J. Hydrometeorol.*, 4, 264–282, 2003.
- White, A. B., Gottas, D. J., Henkel, A. F., Neiman, P. J., Ralph, F. M., and Gutman, S. I.: Developing a performance measure for snow-level forecasts, *J. Hydrometeorol.*, 11, 739–753, doi:10.1175/2009jhm1181.1, 2010.
- Yuter, S. E. and Houze, R. A.: Microphysical modes of precipitation growth determined by S-band vertically pointing radar in orographic precipitation during MAP, *Q. J. Roy. Meteor. Soc.*, 129, 455–476, doi:10.1256/Qj.01.216, 2003.